Tumor eradication in rat glioma and bypass of immunosuppressive barriers using internal radiation with (188)Re-lipid nanocapsules.

Claire Vanpouille-Box, Franck Lacoeuille, Camille Belloche, Nicolas Lepareur,
Laurent Lemaire, Jean-Jacques Le Jeune, Jean-Pierre Benoit, Philippe Menei,
Olivier Couturier, Emmanuel Garcion, et al.

Tumor eradication in rat glioma and bypass of immunosuppressive barriers using internal radiation with [188]Re-lipid nanocapsules

Short title: LNC[188]Re-SSS study using a glioma model

Authors and institutions: Claire Vanpouille-Box[1], Franck Lacoeuille[1,2], Camille Belloche[1], Nicolas Lepareur[3], Laurent Lemaire[1], Jean-Jacques LeJeune[1,2], Jean-Pierre Benoît[1], Philippe Menei[1, 4], Olivier Couturier[1,2], Emmanuel Garcion[1*#], and François Hindré[1*#].

[1]LUNAM Université - INSERM U646 ingénierie de la vectorisation particulaire, 4 rue Larrey, F-49933 Angers cedex 09, France

[2]Nuclear Medicine department, Angers CHU, F-49100, France

[3]Medical imaging departments, CRLCC Eugene Marquis, INSERM U991 foie, métabolisme et cancer, F-35042 Rennes, France – European University of Brittany, F-35000 Rennes, France

[4]Neurosurgery department, Angers CHU, F-49100 Angers, France

*For correspondence or reprints contact: Emmanuel Garcion, Telephone: +33 244 68 85 43; Fax: +33 244 68 85 46; Email: emmanuel.garcion@univ-angers.fr; François Hindré, INSERM U646, Telephone: +33 244 68 85 29; Fax: +33 244 68 85 46; Email: francois.hindre@univ-angers.fr (designed to communicate with the Editorial and Production offices)

#These authors contributed equally to this work.

Key words: rat glioma model, internal radiotherapy, activity gradient, lipid nanocapsules loaded with rhenium-188, adaptative immune response.

ABSTRACT

To date, glioblastoma treatments have only been palliative. In this context, locoregional drug delivery strategies, which allow for blood-brain barrier bypass and reduced systemic toxicity, are of major significance. Recent progress in nanotechnology has led to the development of colloidal carriers of radiopharmaceutics, such as lipid nanocapsules loaded with rhenium-188 (LNC[188]Re-SSS) that are implanted in the brain. In our study, we demonstrated that fractionated internal radiation using LNC[188]Re-SSS triggered remarkable survival responses in a rat orthotopic glioma model (cure rates of 83%). We also highlighted the importance of the radioactivity activity gradient obtained by combining a simple injection (SI) with convection-enhanced delivery (CED). We assumed that the immune system played a role in the treatment's efficacy on account of the overproduction of peripheral cytokines, recruitment of immune cells to the tumor site, and memory response in long-term survivor animals. Hence, nanovectorized internal radiation therapy with activity gradients stimulating immune responses may represent a new and interesting alternative for the treatment of solid tumors such as glioblastomas.

INTRODUCTION

Glioblastomas (GBM) are the most common and lethal type of primary brain tumors [1]. Although surgery and external beam radiation therapy, with or without chemotherapy, slightly improve the prognosis, treatments are never curative [2]. Systemic toxicity, normal brain tissue sensitivity, and the blood-brain barrier (BBB) are the main factors responsible for treatment failure [3].

Ionizing radiation is the gold-standard adjuvant treatment for malignant gliomas. Given that, efforts in developing internal radiation have been made in order to prevent harm to healthy tissues. In this context, locoregional drug delivery modalities, such as stereotactic radiosurgery, which allow for blood-brain barrier (BBB) bypass and reduced systemic toxicity, are of major relevance. Clinical trials on GBM patients supported the usefulness of local radiolabeled peptide receptor therapy (^{90}Y-DOTATOC [4]) and radioimmunotherapy (^{131}I-tenascin antibodies [5] and [188]Re-nimotuzumab [6]). Thus, nanoparticles issued from new technologies hold great promise for developing effective targeted therapies for gliomas. The distribution of the radionuclide will not only depend on its own intrinsic properties but also on those of the vector [7]. Hence, the benefit expected to come from loading the radionuclide is the avoidance of fast elimination after injection.

Colloidal drug carriers have been designed to incorporate radionuclides, such as lipid nanocapsules (LNC). These LNCs are synthesized through a phase inversion process without any organic solvent and consist of a lipid core surrounded by a tensioactive shell [8]. With biomimetic properties, they provide extensive drug encapsulation capacity [9-11] and exhibit biological effects such as P-gp inhibition [12-14], endo-lysosomal escape [15], and biological barrier crossing [15]. LNCs are implanted in brain tumors using stereotactic injections for

locoregional therapy. We recently established the feasibility of this technique using 50nm-LNC loaded with a lipophilic complex of Rhenium-188 (LNC[188]Re-SSS - half-life: 16.9 hours; β⁻ emitter: 2.12 MeV; γ emitter: 155 keV) for internal radiation therapy in malignant glioma, demonstrating a median survival of up to 45 days after a single injection of LNC[188]Re-SSS in an orthotopic 9L-glioma model [9].

In order to optimize internal radiation strategy, we assessed the efficacy of repeated brain administrations of LNC[188]Re-SSS following 9L cell implantation. As simple stereotactic injections (SI) and convection-enhanced delivery (CED) lead to distinct LNC distribution volumes [16], these two LNC[188]Re-SSS infusion techniques were chosen to study the impact of the activity gradient.

The current rationale of ionizing radiation is based on its ability to eradicate tumor cells, notably through excessive reactive oxygen species generation [17, 18]. Nevertheless, several lines of evidence have established that radiotherapy induces dose-dependent consequences such as adaptative responses, genomic instability, and abscopal effects [19-24]. Hence, the recruitment and activation of biological effectors outside the treatment field, notably inflammatory and immune cells such as macrophages [20, 25-27], dendritic cells [28], or T cells, depend on the release of danger signals by irradiated tumor cells and the related microenvironment.

According to the fractionated internal radiotherapy protocol used in our study, different activity gradients may be applied in order to enhance different biologic responses.

In addition, synthetic nano-objects can also function as "danger signals" that activate dendritic cells, potentially inducing subsequent T-cell immunity [29-32]. As gliomas are infiltrative tumors, any modification to the tumor microenvironment via ionizing radiation,

associated with synthetic adjuvants, exemplified by nanoparticles, may aid tumor eradication through both direct and immune-dependent cell death.

Accordingly, we investigated the impact of fractionated internal radiation using LNC[188]Re-SSS on a 9L Fischer rat glioma model. Special attention was given to therapeutic efficiency and the potential involvement of the immune system.

MATERIALS AND METHODS

Ethics Statement

This study was carried out in strict accordance with the French Minister of Agriculture and the European, Communities Council Directive of 24 November 1986 (86/609/EEC). The protocol was approved by the Committee on the Ethics of Animal Experiments of the "Pays de la Loire" (Permit Number: CEEA.2010.3). All surgery was performed under ketamine/xylazine anesthesia, and all efforts were made to minimize suffering.

Materials

Lipoïd® S75-3 (soybean lecithin at 69% of phosphatidylcholine) and Solutol® HS15 (a mixture of polyethylene glycol 660 and polyethylene glycol 660 hydroxystearate) were kindly provided by Lipoïd Gmbh (Ludwigshafen, Germany) and BASF (Ludwigshafen, Germany), respectively. NaCl and dichloromethane were provided by Sigma (St-Quentin, Fallavier, France). Deionized water was obtained from a Milli-Q plus system (Millipore, Paris, France). Lipophilic Labrafac® CC (caprylic-capric acid triglycerides) was provided by Gattefosse S.A. (Saint-Priest, France).

Preparation of the ^{188}Re-SSS complex

^{188}Re as carrier-free Na [^{188}ReO$_4^-$] in physiological solution was obtained by saline elution and concentration of ^{188}W/^{188}Re generator (*Institut des Radioéléments*, Fleurus, Belgium). The

[188]Re-SSS complex was prepared according to the method developed by Lepareur et al. [33].

In brief, the [188]Re-SSS complex was obtained by the reaction of the ligand sodium dithiobenzoate (Plateform of organic synthesis, Rennes, France) with a freeze-dried formulation containing 30mg sodium gluconate, 30mg ascorbic acid, 40mg potassium oxalate, and 4mg $SnCl_2.2H_2O$ reconstituted in 0.5mL of physiological serum. 1 110MBq of [188]Re-perrhenate ([188]ReO_4^-; in 0.5mL) was added, and the solution was mixed for 15 minutes at room temperature. Next, 20mg of sodium dithiobenzoate (in 0.5mL; pH=7) was added before being heated at 100°C for 30 minutes, which allowed for the formation of the [188]Re-SSS complex. Due to its precipitation in aqueous media, the [188]Re-SSS complex was extracted with dichloromethane (1mL) and washed three times with 1mL of deionized water. The radiochemical purity (RCP) of the complex was checked by thin-layer chromatography as the ratio of migrated radioactivity to total radioactivity. Thin-layer chromatography was carried out using silica gel 60-F_{254} alumina plates (Merck) and a solution of petroleum ether/dichloromethane (6/4; v/v) as an eluant. Radioactivity was assessed with a phosphor-imaging machine (Packard, Cyclone storage phosphor system).

Nanocapsule formulation and characterization

The overall study was performed on 50nm diameter LNCs, which were prepared according to a phase-inversion process described by Heurtault et al. [8]. In brief, 25mg Lipoïd® S75-3, 282mg Solutol® HS15, 342.7mg Labrafac®, 29.7mg NaCl, and 987.5mg deionized water were mixed by magnetic stirring. The [188]Re-SSS complex extracted with dichloromethane (1mL) was then added to the other components of the emulsion. The organic solvent was removed

by being heated at 60°C for 15 minutes. Three cycles of progressive heating and cooling between 85°C and 60°C were then carried out and followed by an irreversible shock, induced by dilution with 4.16mL of 0°C deionized water, which was added to the mixture at 70°C. Afterwards, slow magnetic stirring was applied to the suspension for 5 minutes. LNC[188]Re-SSS were dialyzed during 2 hours with deionized water at room temperature by magnetic stirring. The mean diameter and polydispersity index were then determined using a Malvern Zetasizer® Nano Serie DTS 1060 (Malvern Instruments S.A., Worcestershire, UK).

Tumor cells

9L (European Collection of Cell Culture, n° 94110705, Salisbury, UK), a rat gliosarcoma cell line, was maintained in Dulbecco's modified Eagle's medium (DMEM, BioWhittaker, Verviers, Belgium) containing 10% fetal calf serum (FCS) (BioWhittaker, Verviers, Belgium) and 1% antibiotic and antimycotic solution (Sigma, St Quentin Fallavier, France) in a humidified incubator gassed with 5% CO_2 (37°C) until reaching 80–90% confluence. The number of 9L passages at the time of use for the experiments was between P10-P11.

Animals

Female syngeneic Fisher 344 rats aged 9 to 10 weeks were obtained from Charles River (L'arbresle, France). The animals were kept in polycarbonate cages in a room with controlled temperature (20-22°C), humidity (50-70 %), and light (12 hours' light/dark cycles). Room air was renewed at the rate of 10vol/hour. Tap water and diet were provided *ad libitum.*

Intracerebral tumor implantation

Tumor cells for intracerebral implantation were trypsinized, counted, and checked for viability by trypan blue exclusion. Cells were washed twice with Eagle's minimal essential medium (EMEM, BioWhittaker, Verviers, Belgium) without FCS or antibiotics, and a final suspension of $1x10^5$cells/mL in EMEM was obtained. Animals were anesthetized with an intraperitoneal injection of 0.75–1.5mL/kg of a solution containing 2/3 of ketamine (100 mg/mL; Clorketam®, Vétoquinol, Lure, France) and 1/3 xylazine (20mg/mL; Rompun®, Bayer, Puteaux, France). Using a stereotactic head frame and a 10μL Hamilton syringe (Hamilton® glass syringe 700 series RN), 10μL of $1x10^3$9L cells were injected into the rat's right striatum. The coordinates used for the intracerebral injection were 1mm posterior to the bregma, 3mm lateral to the saggital suture (right hemisphere), and 5mm below the dura.

External beam radiation and groups.

An external beam radiation study was performed using a fractionated regimen of 2x8Gy at D6 and D12 following 9L cells implantation. Two groups were studied: a control group (n=6) and a treated one (n=8). We set the therapeutic dose at 16 Gy (2x8Gy) as the maximum tolerated dose (MTD) of 18 Gy (3x6Gy) proved to be effective in the 9L-glioma rat model [34].

Fractionated internal radiation, protocols, and groups

A fractionated internal radiation study was performed at an early and late stage of tumor progression. In the first study, animals underwent internal radiotherapy with 2.8MBq of LNCs loaded with rhenium-188 (LNC[188]Re-SSS) on D6 and D12 following 9L cell implantation. In the second study, the efficacy of LNC[188]Re-SSS was assessed at a late stage of tumor progression, and the animals therefore received internal radiotherapy on D12 and D18. Two different administration types of LNCs (LNC[188]Re-SSS) were chosen: a SI with a final volume of 10μL and a flow of 1μL/min, and a CED injection with a final volume of 60μL and a flow of 0.5μL/min. Depending on the administration technique chosen, four injection protocols were carried out, notably protocol 1: SI at D6 and D12; protocol 2: CED injections at D6 and D12; protocol 3: CED injection at D6 (or D12) and SI at D12 (or D18); protocol 4: SI at D6 (or D12) and CED injection at D12 (or D18). Each protocol was composed of four groups: a LNC[188]Re-SSS group (n=6), a blank LNC group (n=4), a $^{188}ReO_4^-$ group (n=4), and a saline solution group (n=4).

We chose to set the injected activity at 2.8 MBq of LNC[188]Re-SSS because it proved to be effective after a single injection in the 9L-glioma model [9].

Simple injection and convection enhancement delivery procedures

The animals were anesthetized with an intraperitoneal injection of 0.75–1.5mL/Kg of a solution containing 2/3 of ketamine (100mg/mL; Clorketam®, Vétoquinol, Lure, France) and 1/3 xylazine (20mg/mL; Rompun®, Bayer, Puteaux, France). For the SI, 10μL were injected

into the rat striatum at a flow of 1µL/min using a 10µL syringe (Hamilton® glass syringe 700 series RN) with a 32-G needle (Hamilton ®). For this purpose, rats were immobilized in a stereotactic head frame (Lab Standard Stereotactic; Stoelting, Chicago, IL). Coordinates were 1mm posterior to the bregma, 3mm lateral to the saggital suture, and 5mm below the dura. Following the injection, the needle was left in place for an additional 5 minutes to avoid expulsion of the suspension from the brain during the removal of the syringe.

CED injection was similar, except that the 10µL Hamilton® syringe with a 32-G needle was connected to a 100µL Hamilton ® 22-G syringe containing the product (Harvard Apparatus, Les Ulis, France) through a cannula (CoExTMPE/PVC tubing, Harvard Apparatus, Les Ulis, France). CED was performed using an osmotic pump PHD 2,000 infusion (Harvard Apparatus, Les Ulis, France) by controlling a 0.5µL/min rate for 2 hours.

Tissue distribution study

A tissue distribution study was carried out using 16 female Fisher rats 6 days following 9L implantation. They were divided into two groups: one injected with LNC[188]Re-SSS after a SI (n=8) and one with LNC[188]Re-SSS following a CED injection (n=8). In both groups, the animals were sacrificed at post-injection interval times of 24 hours (n=4) and 96 hours (n=4). The organs were removed, washed, and weighed (blood, liver, spleen, kidneys, heart, lung, stomach, small intestine, large intestine, bladder, bone, muscle, brain, and carcass). The content activity of each organ was determined using a gamma counter (Packard Auto-Gamma 5,000 series).

Autoradiography

Female Fisher rats 6 days following 9L cell implantation received 2.8MBq after SI and CED injections of LNC[188]Re-SSS (n=3 per group). Twenty-four hours following the LNC[188]Re-SSS injection, the brain was extracted and fixed with 4% of paraformaldehyde in phosphate-buffered saline 1X (pH=7.3). Coronal sections (1mm thick) were prepared from brains on an acrylic brain matrix. Brain slices were then placed on phosphor screens for 1 minute and read by the Cyclone Phosphor Imaging System (Packard Instruments).

MRI

MRI was performed with a Bruker Avance DRX 300 (Germany) machine equipped with a magnet of 7T. Rapid T2-weighted images were obtained using rapid acquisition with relaxation enhancement (RARE) sequence (TR=2,000ms; mean echo time [Tem]=31.7ms; RARE factor=8; FOV=3x3cm; matrix 128x128; nine contiguous slices of 1mm; eight acquisitions).

Interleukin-2 (IL-2) and interferon-γ (IFN$_γ$) quantifications

Blood samples were collected from the tail vein using heparinized tubes in each protocol from a fractionated internal radiation study (D6/D12) at D8, D16, and D24 following 9L cell implantation. After centrifugation at 1 000g for 20 minutes, the rat IL-2 and rat IFN$_γ$ ELISA tests (Duoset, R&D Systems Europe, Lille, France) were immediately performed according to manufacturer's instructions.

Immunohistochemistry

Brains from tumor-bearing animals treated were frozen at D15, D24, and D32 in isopentane cooled by liquid nitrogen and stored at -80°C. Fourteen-micron cryosections were fixed with 4% of paraformaldehyde in phosphate-buffered saline 1X (pH=7.3) and washed three times with phosphate-buffered saline (PBS). In order to block nonspecific binding, sections were incubated 1 hour in PBS containing 4% BSA and 10% normal goat serum, and washed twice with PBS. All incubations with primary antibodies (OX18 antibody: mouse, 1/100, BD Sciences; OX6 antibody: mouse, 1/100, BD Sciences; OX62 antibody: mouse, 1/100, BD Sciences; CD161a antibody: mouse, 1/100, BD Sciences; OX42 antibody: mouse, 1/100, BD Sciences; CD4 antibody: mouse, 1/100, BD Sciences; CD8b antibody: mouse, 1/100, BD Sciences; and IgG isotypes) were performed overnight at 4°C at a 1/100 final dilution. Primary antibodies were detected using a rat-absorbed biotinylated anti-mouse IgG secondary antibody (BD Biosciences). After 1 hour of incubation at 4°C, the sections were washed twice with PBS containing 4% of BSA. Sections were developed with Alexa 488-conjugated secondary antibody (Streptavidin Alexa Fluor 488 conjugate S11223, Invitrogen) at a final concentration of 2.5µg/mL after an incubation of 1 hour at 4°C and washed four times with PBS 1X. After immunostaining, DAPI (4', 6-diamidino-2-phenylindole dihydrochloride D9542, 0.1µg/mL, Sigma, St Quentin Fallavier, France) was added for 20 minutes at room temperature to stain the nuclei.

Re-challenging

Long-term survivors obtained from fractionated internal radiation studies (D6/D12 and D12/D18) were re-challenged with 1 000 9L cells in the left striatum. The animals were anesthetized with an intraperitoneal injection of 0.75 – 1.5mL/kg of a solution containing 2/3 of ketamine (100mg/mL; Clorketam®, Vétoquinol, Lure, France) and 1/3 xylazine (20mg/mL; Rompun®, Bayer, Puteaux, France). The intracerebral tumor implantation procedure was described above, but the coordinates used were modified: 1mm posterior to the bregma, 3mm lateral to the saggital suture (left hemisphere), and 5mm below the dura.

Statistical analysis

Results are expressed as mean±standard deviation (SD). For the survival study, comparisons between control groups were made using the log-rank test (Mantel-Cox test). For other studies, statistical analysis was performed using the *t* test. Data was considered to be significant when $p < 0.05$.

RESULTS

Biodistribution of nanovectorized radionuclide: importance of the administration route

In order to highlight the importance of the administration route, biodistribution of LNC^{188}Re-SSS was assessed. At Day 6 following 9L cell implantation, we examined the usefulness of encapsulating rhenium-188 within LNCs in order to maintain high levels of radiopharmaceutics in the brain. Rhenium-188 entrapping is essential, as only 4% and 65% of the injected dose were eliminated in urine and feces, respectively, 96 hours after injecting LNC^{188}Re-SSS and the solution of ^{188}Re-perrhenate (^{188}ReO$_4^-$) (Figure 1a). Depending on the rhenium-188 formulation, different distributions were obtained, whereas the two administration techniques (SI; CED) had no impact on the elimination process (Figures 1b-c). This was corroborated by biodistribution studies, with 86% and 78% of the injected dose remaining in the brain 24 hours and 96 hours post-injection, respectively, regardless of the administration technique used (Figure 1d).

Importance of the administration route on the activity gradient

To address the distribution of LNC^{188}Re-SSS within the brain, autoradiography views were performed 24 hours after SI and CED injections (Figure 1e-g). Even if biodistributions were similar using SI or CED injections, the distribution within the brain tissue itself revealed the rhenium-188 spread to be greater with CED than SI administrations, as illustrated by LNC^{188}Re-SSS areas of 34.74±0.72mm² and 21.57±0.78mm², respectively (p=0.00004) (Figure 1e,f). Relative radioactivity was quantified using OptiQuant software and expressed as the mean radioactivity density (DLU/mm²). Results revealed the radioactivity content to be more

concentrated for the SI injection compared to the CED, with 64.54±1.99DLU/mm² and 23.24±2.68 DLU/mm², respectively (p=0.0006) (Figure 1e,g).

Treatment efficacy of fractionated internal radiotherapy at Day 6 and Day 12 following tumor implantation

In addition to characterizing the LNC[188]Re-SSS distribution, the efficacy of fractionated internal radiation therapy was studied. Rats were treated with stereotactic injections of 2.8MBq of LNC[188]Re-SSS 6 days (D6) and 12 days (D12) after 9L cell implantation. Depending on the administration technique (SI or CED), four injection protocols were used, notably protocol 1: SI at D6 and D12; protocol 2: CED at D6 and D12; protocol 3: CED at D6 and SI at D12; protocol 4: SI at D6 and CED at D12. In control group animals, the median survival time was close to 30 days for $^{188}ReO_4^-$ and 28 days for both blank LNC and saline solutions (Figures 2a-d). There were no significant differences between the control groups (p>0.05), regardless of the injection protocol used. Treatments with LNC[188]Re-SSS were associated with an increased median survival time (IMST) of 37.5% and 35.7% for protocols 1 and 2, with 13% and 0% of long-term survivors, respectively (Figures 2a-b). Long-term survivors were defined as animals that survived for more than 120 days following 9L cell implantation [35]. Magnetic resonance imaging [36] corroborated this observation, with no tumor progression revealed. The combination of CED and SI strongly improved animal survival, with an IMST of 176% with protocol 3 and 257% with protocol 4 (Figure 2c-d). Combining the two administration types exhibiting distinct activity gradients had a strong impact on survival (7 out of 12 animals were long-term survivors for protocols 3 and 4 versus only one out of 12 for protocols 1 and 2). MRI follow-up, which is able to detect

9L glioma tumors from Day 9, confirmed these findings with similar tumor progression in the control groups, as demonstrated by representative images obtained with physiological serum (Figure 2e). Protocols 1 and 2 led to a comparable evolution with a slightly delayed tumor progression. In contrast, protocols 3 and 4 resulted in tumor eradication (Figure 2e).

Treatment efficacy of fractionated internal radiotherapy after tumor detection (D12/D18)

In order to mimic late-stage tumor progression, fractionated internal radiation was performed at D12 and D18 following 9L cell implantation. Protocols 3 and 4, which provided the best survival results during prior treatment, were used. As expected, no significant differences between the control groups were detected, with a median survival close to 28 days. However, with protocols 3 and 4, five out of six rats (83%) were long-term survivors (Figures 2f-g). MRI confirmed these results, with a tumor lesion at D9 following 9L cell implantation, which grew up until D25 and then regressed, long-term survivor animals being free of brain tumors (Figure 2h).

Effect of LNC^{188}Re-SSS on the production of peripheral cytokines

As over-expression of interleukin-2 (IL-2) and interferon-γ (IFNγ) cytokines produced by T cells are important for anti-tumoral brain immune reponses [37], these cytokines were quantified at D8, D16, and D24 in blood of control and LNC^{188}Re-SSS-treated animals for protocols 3 and 4 (Figures 3a-b). No significant differences between the control groups were observed (saline solution, blank LNC, and ^{188}ReO$_4^-$ solution); hence results of control groups

were expressed as a mean ± standard deviation of all control groups data. LNC[188]Re-SSS treatment resulted in an overproduction of peripheral cytokines, as major increases in IL-2 and IFNγ were observed in LNC[188]Re-SSS groups.

Recruitment and activation of immune and inflammatory cells within the central nervous system after LNC[188]Re-SSS treatment

In order to evaluate immunostimulating effects of LNC[188]Re-SSS versus blank LNC, the immunostaining of central nervous system (CNS) infiltrating or resident immune cells was assessed and illustrated for protocol 4, with results similar to those observed in protocol 3 (Figures 4a-b). Immunostaining of brain cryosections at D15 demonstrated a stronger activation of monocyte-macrophage-microglia in LNC[188]Re-SSS-treated animals, as proven by the ameboid shape of OX42-positive cells [38, 39]. In addition, an improved recruitment of natural killer (CD161a) and dendritic cells (OX62) was observed from D15 to D25, with a slight decrease at D32.

MHC class II (OX6) over-expression in LNC[188]Re-SSS-treated rats confirmed the recruitment and activation of inflammatory and immune cells in the CNS. Strong induction of MCH class I (OX18), whether present on the glioma cells themselves or on antigen-presenting cells, provided evidence in favor of an improved capability to develop an antitumor immune response. As effectors of the antitumor immune response, such as CD4 and CD8 positive cells, were absent at D15, they were progressively recruited in the CNS tumors at D25 and D32 (Figures 4a-b).

Rechallenge in long-term survivors reveals immune protection

To validate this immune response, long-term animal survivors obtained with protocols 3 and 4 were re-challenged with implantation of 1 000 9L cells in the left striatum. Regardless of the fractionated internal radiation timing used (D6/D12, Figure 5a; D12/D18, Figure 5b), median survival was significantly improved (from 35 to 37 days) when compared to control animals (25 days). Moreover, one long-term survivor was obtained for treatment at D6/D12 with protocol 4 and for treatment at D12/18 with protocols 3 and 4, thus representing three of 17 animals included in the study.

Treatment efficacy of fractionated external beam radiation at Day 6 and Day 12 following tumor implantation and its immune system effect

External beam radiation was performed and its related-biological effect assessed in order to compare our internal radiation strategy with routine treatment. Rats were treated with 2 x 8 Gy regimen at Day 6 and Day 12 following 9L cell implantation. External beam radiation efficacy resulted in a slight increase with a median survival of 26.5±2.1 days and 33.5±1.5 days for control and treated animals, respectively (Figure 6a,b). Meanwhile, the immunostaining of CNS infiltrating or resident immune cells revealed a weaker recruitment of immune cells, in particular natural and dendritic cells, which are crucial in adaptative immune responses (Figure 6c,d).

DISCUSSION

In this study, we evaluated fractionated internal radiation therapy using LNC[188]Re-SSS in an orthotopic 9L Fischer rat glioma model. Survival and immune-related effects induced by the variation in the [188]Re-activity gradient within the brain parenchyma were investigated.

The first part of this work highlights the advantages of using LNC for entrapping Rhenium-188 as physico-chemical properties of the nanocarrier prevail over those of Rhenium-188. Hence, our data supported that most of rhenium-188 activity from LNC remained confined to the brain until its disintegration.

The originality of our strategy was to use two modes of stereotaxic injections during the fractionated treatment in order to modulate [188]Re distribution within the brain. Thus, a remarkable survival benefit was only revealed when SI injection was combined with CED, indicating that the [188]Re-activity gradient is of major significance. This therapeutic effect can be explained by the cellular heterogeneity and the related microenvironment of the tumor mass. Solid tumors are indeed heterogenous from a histology point of view with inflammatory infiltrates and vascular structures [40]. Different subpopulations of cancer cells are hierarchically and topographically organized, with radio-resistant cancer initiating cells [41] within either hypoxic or vascular niches [42]. Thus, we can assume that the injection of LNC[188]Re-SSS by the combination of SI and CED injections targets different types of radiosensitive and radioresistant sub-cellular populations within the tumor mass. As it is more difficult to apply an activity-gradient irradiation within the tumor mass through external beam radiation, being the gold-standard adjuvant treatment for gliomas, these possibilities are important to consider. Corroborating this idea, the fractionated external

beam radiation used in this study triggered weaker therapeutic efficiency as compared with internal radiotherapy.

In this study, animals were treated with a combination of SI and CED at Days 6/12 and 12/18 following 9L cells implantation. As no significant differences were noted between early- and late-care of the tumor, tumor size and proliferation gradient did not appear to influence treatment response. This could be explained by a [188]Re-activity gradient that is sufficient for direct eradication of the entire tumor mass in the two situations (early- and late-care). In addition, the [188]Re-activity gradient might induce an indirect immune response likely to affect all types of tumor cells. Thus, we have investigated whether an adaptative immune response was involved in tumor regression. According to the scientific literature, radiation after external beam radiation exposure produces an immunogenic death of the most radiosensitive subset of cancer cells [43]. Recent evidence has highlighted the involvement of calreticulin and high-mobility group protein B1 (HMGB1) in the mechanism by which the irradiated tumor can become a source of antigen [19, 44]. Our data demonstrated that while there was a recruitment of immune cells with both internal and external radiotherapy, the intensity of this response was weaker after external than internal radiation. In addition, our internal radiation strategy induced a memory antitumor response as long-term survivors were partially or totally immunized after re-injecting 9L cells in contrast to naïve animals. As no long-term survivor animals were obtained with external beam radiation, the intensity of the immune response depending on the irradiation mode may play a role. Radiation has been reported to induce up-regulation of MCHI and other pro-immunogenic effects at the irradiated site [21, 45]. As MCHI expression was more important after internal radiotherapy compared with external radiation modality, we assume that tumor cell recognition by the

immune system is improved in this context. Moreover, Dewan et al. have shown that two external radiation regimens had similar effects on tumor growth, but led to different synergistic effects when associated with immunotherapy [46]. The conditions of irradiation are of major significance, and the ^{188}Re-activity gradient used in our study may well play a role by enhancing a particular type of cell death (apoptosis, autophagy, or necrosis), thus leading to tumor eradication or not [47].

The nano-object used for internal radiotherapy can interact with immune responses. As previously shown in scientific literature, the transporters associated with antigen processing (TAP) and multidrug resistance efflux pumps share a significant degree of homology among their transmembrane domains, which are thought to be the primary determinants of substrate specificity [48, 49]. As nanoparticles interfere with P-gp and reverse multidrug resistance in glioma cells [12], they could promote pro-immunogenic conditions by increasing antigen processing based on interactions with TAP transporters. LNC may also cross biological barriers [12] with endo-lysosomal escape [15], which may impact autophagy cell death [50]. This could be crucial as migrating glioblastoma cells have been shown to be resistant to apoptosis [50].

CONCLUSION

Fractionated internal radiotherapy using LNC[188]Re-SSS induced a remarkable survival benefit in rat glioma model, with a significant increase in the number of long-term survivor animals. Those observations are mainly ascribed to [188]Re-activity gradient leading to a bypass of immunosuppressive barriers, thus demonstrated by total or partial immunity of rechallenged animals. Hence, the present work strengthen the interest of developing new anti-glioblastoma strategies based on internal radiotherapy using [188]Re-lipid nanocapsules associated with immunotherapy.

REFERENCES

[1] Bondy ML, Scheurer ME, Malmer B, Barnholtz-Sloan JS, Davis FG, Il'yasova D, et al. Brain tumor epidemiology: consensus from the Brain Tumor Epidemiology Consortium. Cancer. 2008;113:1953-68.

[2] Stupp R, Mason WP, van den Bent MJ, Weller M, Fisher B, Taphoorn MJ, et al. Radiotherapy plus concomitant and adjuvant temozolomide for glioblastoma. N Engl J Med. 2005;352:987-96.

[3] Muldoon LL, Soussain C, Jahnke K, Johanson C, Siegal T, Smith QR, et al. Chemotherapy delivery issues in central nervous system malignancy: a reality check. J Clin Oncol. 2007;25:2295-305.

[4] Schumacher T, Hofer S, Eichhorn K, Wasner M, Zimmerer S, Freitag P, et al. Local injection of the 90Y-labelled peptidic vector DOTATOC to control gliomas of WHO grades II and III: an extended pilot study. Eur J Nucl Med Mol Imaging. 2002;29:486-93.

[5] Reardon DA, Quinn JA, Akabani G, Coleman RE, Friedman AH, Friedman HS, et al. Novel human IgG2b/murine chimeric antitenascin monoclonal antibody construct radiolabeled with 131I and administered into the surgically created resection cavity of patients with malignant glioma: phase I trial results. J Nucl Med. 2006;47:912-8.

[6] Casaco A, Lopez G, Garcia I, Rodriguez JA, Fernandez R, Figueredo J, et al. Phase I single-dose study of intracavitary-administered Nimotuzumab labeled with 188 Re in adult recurrent high-grade glioma. Cancer Biol Ther. 2008;7:333-9.

[7] Caruthers SD, Wickline SA, Lanza GM. Nanotechnological applications in medicine. Curr Opin Biotechnol. 2007;18:26-30.

[8] Heurtault B, Saulnier P, Pech B, Proust JE, Benoit JP. A novel phase inversion-based process for the preparation of lipid nanocarriers. Pharm Res. 2002;19:875-80.

[9] Allard E, Hindre F, Passirani C, Lemaire L, Lepareur N, Noiret N, et al. 188Re-loaded lipid nanocapsules as a promising radiopharmaceutical carrier for internal radiotherapy of malignant gliomas. Eur J Nucl Med Mol Imaging. 2008;35:1838-46.

[10] Hureaux J, Lagarce F, Gagnadoux F, Vecellio L, Clavreul A, Roger E, et al. Lipid nanocapsules: ready-to-use nanovectors for the aerosol delivery of paclitaxel. Eur J Pharm Biopharm. 2009;73:239-46.

[11] Vonarbourg A, Passirani C, Desigaux L, Allard E, Saulnier P, Lambert O, et al. The encapsulation of DNA molecules within biomimetic lipid nanocapsules. Biomaterials. 2009;30:3197-204.

[12] Garcion E, Lamprecht A, Heurtault B, Paillard A, Aubert-Pouessel A, Denizot B, et al. A new generation of anticancer, drug-loaded, colloidal vectors reverses multidrug resistance in glioma and reduces tumor progression in rats. Mol Cancer Ther. 2006;5:1710-22.

[13] Lamprecht A, Benoit JP. Etoposide nanocarriers suppress glioma cell growth by intracellular drug delivery and simultaneous P-glycoprotein inhibition. J Control Release. 2006;112:208-13.

[14] Roger E, Lagarce F, Garcion E, Benoit JP. Reciprocal competition between lipid nanocapsules and P-gp for paclitaxel transport across Caco-2 cells. Eur J Pharm Sci. 2010;40:422-9.

[15] Paillard A, Hindre F, Vignes-Colombeix C, Benoit JP, Garcion E. The importance of endo-lysosomal escape with lipid nanocapsules for drug subcellular bioavailability. Biomaterials. 2010;31:7542-54.

[16] Vinchon-Petit S, Jarnet D, Paillard A, Benoit JP, Garcion E, Menei P. In vivo evaluation of intracellular drug-nanocarriers infused into intracranial tumours by convection-enhanced delivery: distribution and radiosensitisation efficacy. J Neurooncol.97:195-205.

[17] Bucci B, Misiti S, Cannizzaro A, Marchese R, Raza GH, Miceli R, et al. Fractionated ionizing radiation exposure induces apoptosis through caspase-3 activation and reactive oxygen species generation. Anticancer Res. 2006;26:4549-57.

[18] Guo G, Yan-Sanders Y, Lyn-Cook BD, Wang T, Tamae D, Ogi J, et al. Manganese superoxide dismutase-mediated gene expression in radiation-induced adaptive responses. Mol Cell Biol. 2003;23:2362-78.

[19] Apetoh L, Ghiringhelli F, Tesniere A, Obeid M, Ortiz C, Criollo A, et al. Toll-like receptor 4-dependent contribution of the immune system to anticancer chemotherapy and radiotherapy. Nat Med. 2007;13:1050-9.

[20] Coates PJ, Rundle JK, Lorimore SA, Wright EG. Indirect macrophage responses to ionizing radiation: implications for genotype-dependent bystander signaling. Cancer Res. 2008;68:450-6.

[21] Formenti SC, Demaria S. Systemic effects of local radiotherapy. Lancet Oncol. 2009;10:718-26.

[22] Galluzzi L, Maiuri MC, Vitale I, Zischka H, Castedo M, Zitvogel L, et al. Cell death modalities: classification and pathophysiological implications. Cell Death Differ. 2007;14:1237-43.

[23] Larsson M, Fonteneau JF, Bhardwaj N. Dendritic cells resurrect antigens from dead cells. Trends Immunol. 2001;22:141-8.
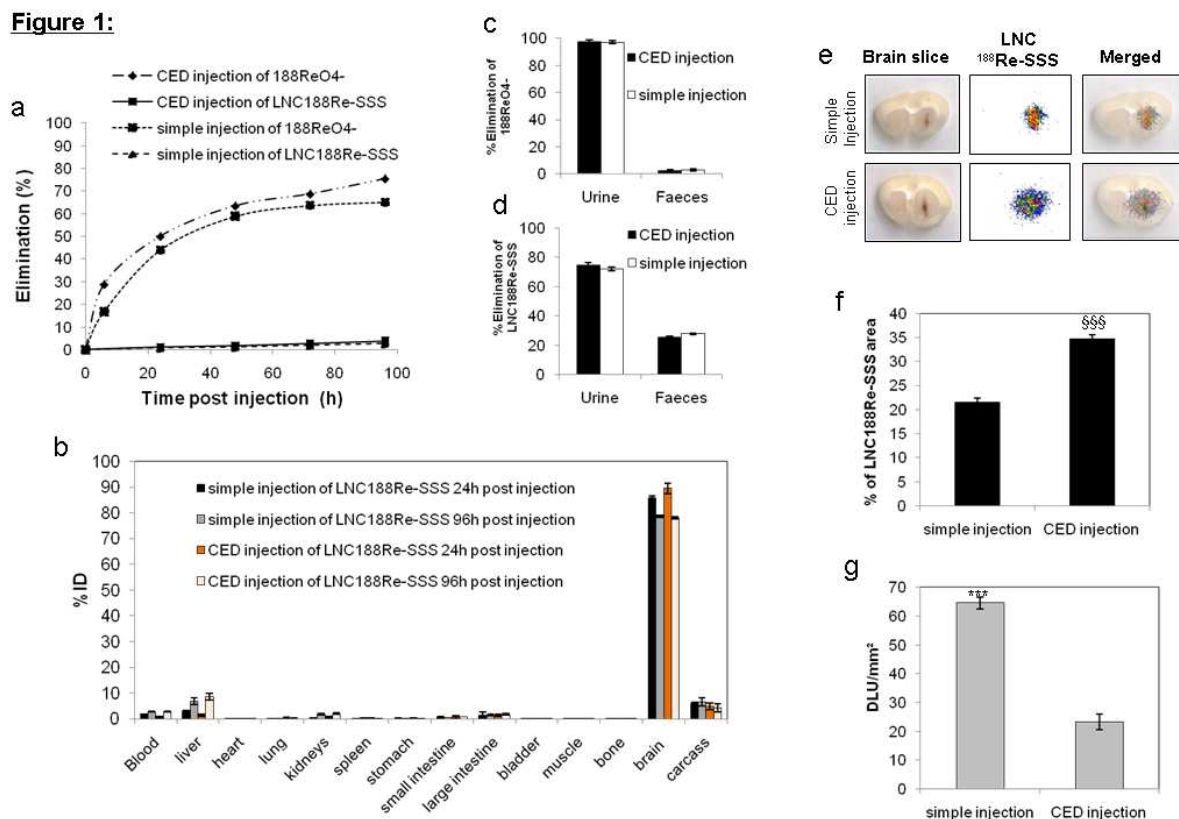
[24] Pasi F, Facoetti A, Nano R. IL-8 and IL-6 bystander signalling in human glioblastoma cells exposed to gamma radiation. Anticancer Res. 2010;30:2769-72.

[25] Hallahan DE, Spriggs DR, Beckett MA, Kufe DW, Weichselbaum RR. Increased tumor necrosis factor alpha mRNA after cellular exposure to ionizing radiation. Proc Natl Acad Sci U S A. 1989;86:10104-7.

[26] Hong JH, Chiang CS, Tsao CY, Lin PY, McBride WH, Wu CJ. Rapid induction of cytokine gene expression in the lung after single and fractionated doses of radiation. Int J Radiat Biol. 1999;75:1421-7.

[27] McBride WH, Chiang CS, Olson JL, Wang CC, Hong JH, Pajonk F, et al. A sense of danger from radiation. Radiat Res. 2004;162:1-19.

[28] Roses RE, Xu M, Koski GK, Czerniecki BJ. Radiation therapy and Toll-like receptor signaling: implications for the treatment of cancer. Oncogene. 2008;27:200-7.

[29] Bennewitz NL, Babensee JE. The effect of the physical form of poly(lactic-co-glycolic acid) carriers on the humoral immune response to co-delivered antigen. Biomaterials. 2005;26:2991-9.

[30] Hunter R, Strickland F, Kezdy F. The adjuvant activity of nonionic block polymer surfactants. I. The role of hydrophile-lipophile balance. J Immunol. 1981;127:1244-50.

[31] Reddy ST, Swartz MA, Hubbell JA. Targeting dendritic cells with biomaterials: developing the next generation of vaccines. Trends Immunol. 2006;27:573-9.

[32] Yoshida M, Babensee JE. Poly(lactic-co-glycolic acid) enhances maturation of human monocyte-derived dendritic cells. J Biomed Mater Res A. 2004;71:45-54.

[33] Lepareur N NNaHJ. A kit formulation for the labelling of lipiodol with generator-produced 188Re. Journal of Labelled Compounds and Radiopharmaceuticals. 2004;47:857-67.

[34] Vinchon-Petit S, Jarnet D, Jadaud E, Feuvret L, Garcion E, Menei P. External irradiation models for intracranial 9L glioma studies. J Exp Clin Cancer Res. 2010;29:142.

[35] Recinos VR, Tyler BM, Bekelis K, Sunshine SB, Vellimana A, Li KW, et al. Combination of intracranial temozolomide with intracranial carmustine improves survival when compared with either treatment alone in a rodent glioma model. Neurosurgery. 2010;66:530-7; discussion 7.

[36] Brady LW, Miyamoto C, Woo DV, Rackover M, Emrich J, Bender H, et al. Malignant astrocytomas treated with iodine-125 labeled monoclonal antibody 425 against epidermal growth factor receptor: a phase II trial. Int J Radiat Oncol Biol Phys. 1992;22:225-30.

[37] Roth W, Weller M. Chemotherapy and immunotherapy of malignant glioma: molecular mechanisms and clinical perspectives. Cell Mol Life Sci. 1999;56:481-506.

[38] Bhat R, Steinman L. Innate and adaptive autoimmunity directed to the central nervous system. Neuron. 2009;64:123-32.

[39] Carpentier PA, Palmer TD. Immune influence on adult neural stem cell regulation and function. Neuron. 2009;64:79-92.

[40] Adams JM, Strasser A. Is tumor growth sustained by rare cancer stem cells or dominant clones? Cancer Res. 2008;68:4018-21.

[41] Bao S, Wu Q, McLendon RE, Hao Y, Shi Q, Hjelmeland AB, et al. Glioma stem cells promote radioresistance by preferential activation of the DNA damage response. Nature. 2006;444:756-60.
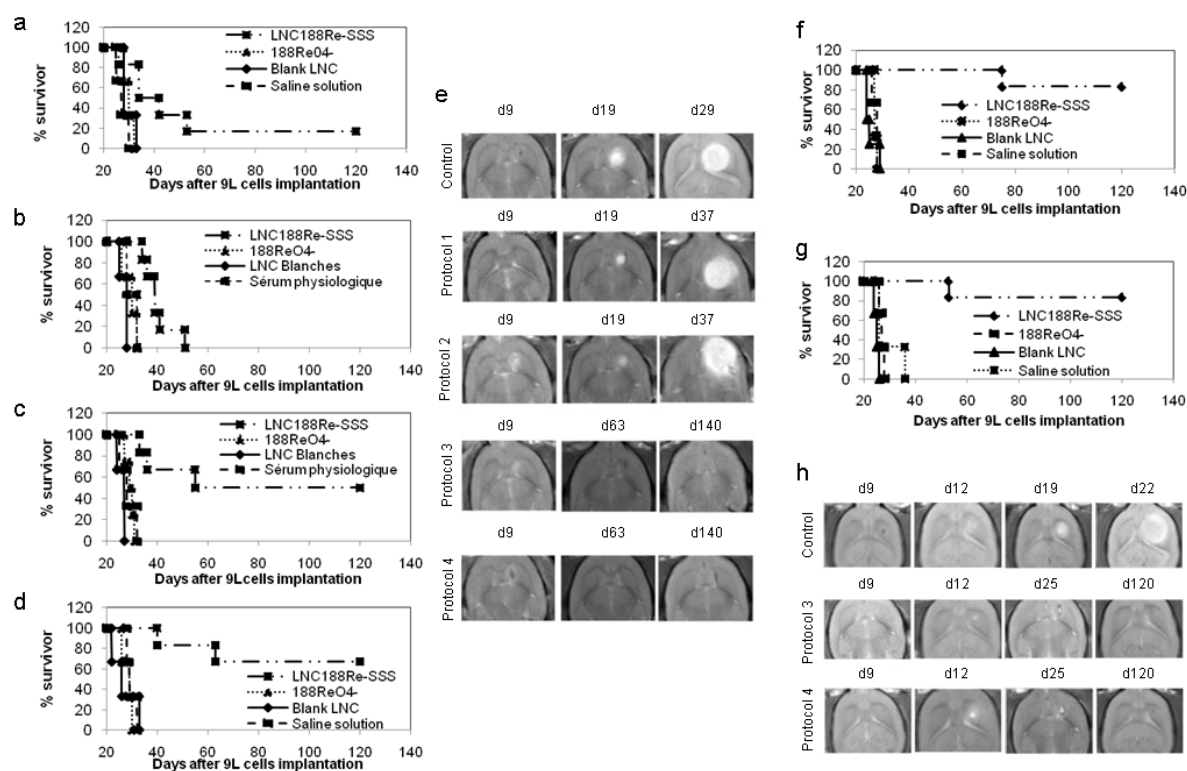
[42] Rich JN. Cancer stem cells in radiation resistance. Cancer Res. 2007;67:8980-4.

[43] Obeid M, Panaretakis T, Joza N, Tufi R, Tesniere A, van Endert P, et al. Calreticulin exposure is required for the immunogenicity of gamma-irradiation and UVC light-induced apoptosis. Cell Death Differ. 2007;14:1848-50.

[44] Obeid M, Tesniere A, Ghiringhelli F, Fimia GM, Apetoh L, Perfettini JL, et al. Calreticulin exposure dictates the immunogenicity of cancer cell death. Nat Med. 2007;13:54-61.

[45] Chakraborty M, Abrams SI, Coleman CN, Camphausen K, Schlom J, Hodge JW. External beam radiation of tumors alters phenotype of tumor cells to render them susceptible to vaccine-mediated T-cell killing. Cancer Res. 2004;64:4328-37.

[46] Dewan MZ, Galloway AE, Kawashima N, Dewyngaert JK, Babb JS, Formenti SC, et al. Fractionated but not single-dose radiotherapy induces an immune-mediated abscopal effect when combined with anti-CTLA-4 antibody. Clin Cancer Res. 2009;15:5379-88.

[47] Demaria S, Pikarsky E, Karin M, Coussens LM, Chen YC, El-Omar EM, et al. Cancer and inflammation: promise for biologic therapy. J Immunother. 2010;33:335-51.

[48] Izquierdo MA, Neefjes JJ, Mathari AE, Flens MJ, Scheffer GL, Scheper RJ. Overexpression of the ABC transporter TAP in multidrug-resistant human cancer cell lines. Br J Cancer. 1996;74:1961-7.

[49] Manavalan P, Smith AE, McPherson JM. Sequence and structural homology among membrane-associated domains of CFTR and certain transporter proteins. J Protein Chem. 1993;12:279-90.

[50] Lefranc F, Kiss R. Autophagy, the Trojan horse to combat glioblastomas. Neurosurg Focus. 2006;20:E7.

ACKNOWLEDGEMENTS

Figure 1: **Distribution of LNCs loaded with rhenium-188**

a: [188]Re elimination measured in urine and feces by a gamma counter during 96 hours following SI and CED injections of $^{188}ReO_4^-$ and LNC^{188}Re-SSS in 9L glioma-bearing rats 6 days following 9L implantation. Repartition between urine and feces for $^{188}ReO_4^-$. (**b**) and LNC^{188}Re-SSS (**c**). **d**: Organ biodistribution of $^{188}ReO_4^-$ (n=8) and LNC^{188}Re-SSS (n=8) solutions 24 and 96 hours after the injection; results are expressed as a percentage of the injected dose per gram of organ, mean±SD. **e**: Autoradiography views of LNC^{188}Re-SSS injected by SI and CED injections 24 hours following the injection. **f**: Relative amount of radioactivity in brain slices after bolus and CED injections of LNC^{188}Re-SSS. **g**: Percentage of LNC^{188}Re-SSS area after bolus and CED injections

Figure 2:

Figure 2: Efficacy of fractionated internal radiation with LNCs loaded with rhenium-188

a-d: Kaplan-Meier survival curves of rats treated at D6 and D12, 5.6MBq of LNC^{188}Re-SSS (n=6), 5.6MBq of ^{188}ReO$_4^-$ (n=4), blank LNC (n=4), and saline solution (n=4). **a**: Protocol 1, SI at D6 and D12. One in six rats was a long-term survivor (>120 days). **b**: Protocol 2, CED injections at D6 and D12. **c**: Protocol 3, CED and SI at D6 and D12. Three in six rats were long-term survivors. **d**: Protocol 4, SI and CED injections at D6 and D12. Four in six rats were long-term survivors. **e**: T2-weighted images of control rats and LNC^{188}Re-SSS in each protocol of the D6/D12 fractionated internal study. **f-g**: Kaplan-Meier survival curves of rats treated at D12 and D18, 5.6MBq of LNC^{188}Re-SSS (n=6), 5.6MBq of ^{188}ReO$_4^-$ (n=4), blank LNC (n=4), and saline solution (n=4). **f**: Protocol 3, CED and SIs at D12 and D18. Five in six rats were long-term survivors. **g**: Protocol 4, SI at D12 and CED injection at D18. Five in six rats were long-term survivors. **h**: T2-weighted images of control rats and LNC^{188}Re-SSS in each protocol of the D12/D18 fractionated internal study
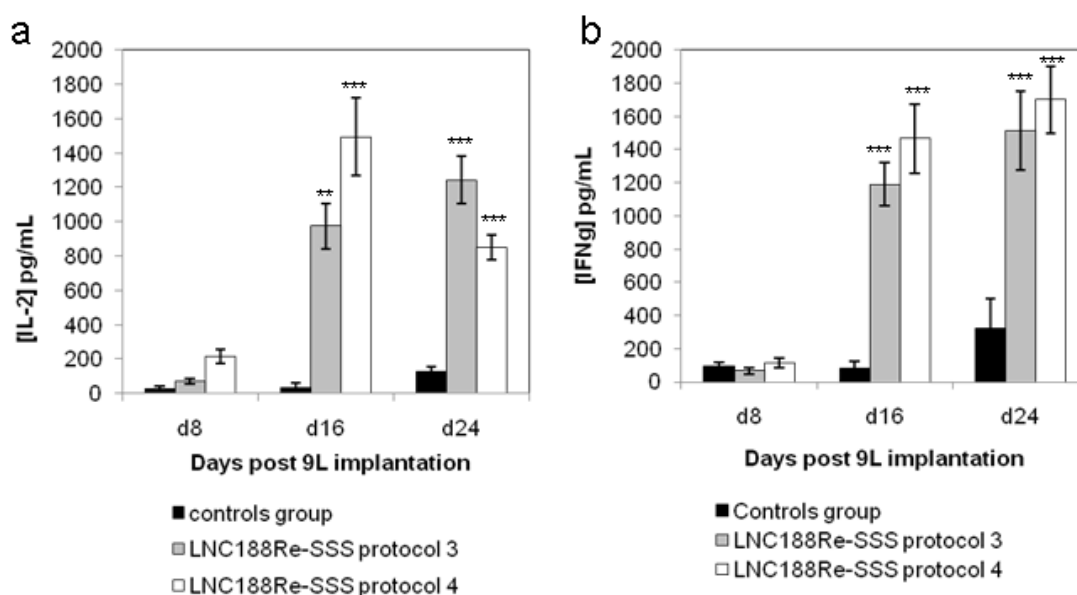
Figure 3

Figure 3: Peripheral cytokines (interleukin-2 and interferon-) quantification after nanovectorized internal radiotherapy

Concentrations of interleukin-2 (IL-2) (**a**) and interferon-γ (IFNγ) (**b**) for control group and LNC[188]Re-SSS of each protocol. Results are expressed in pg/mL of IL-2 and IFNγ, mean±SD. Comparison of IL-2 content in LNC[188]Re-SSS groups versus control groups; **p<0.01; ***p<0.001
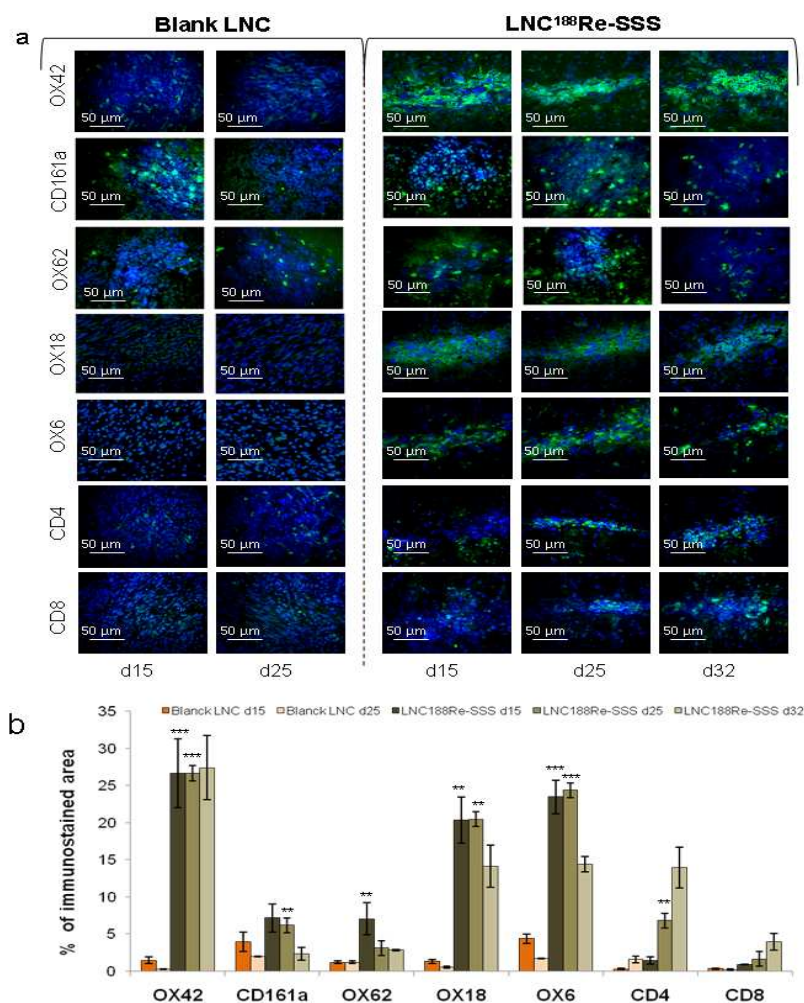
Figure 4

Figure 4: **Recruitment and activation of immune and inflammatory cells within the central nervous system after LNC^{188}Re-SSS treatment**

a: Immunohistochemistry staining of macrophage cells (OX42), natural killer cells (OX61), major histocompatibility (class I - OX18; class II – OX6), dendritic cells (CD161a), and T lymphocytes cells (CD4 and CD8) of protocol 3 and 4 of the D6/D12 fractionated study. **b**: Semi-quantitative results of immunohistochemistry. Results are expressed as % of immunostaining area after their determination with MetaMorph software
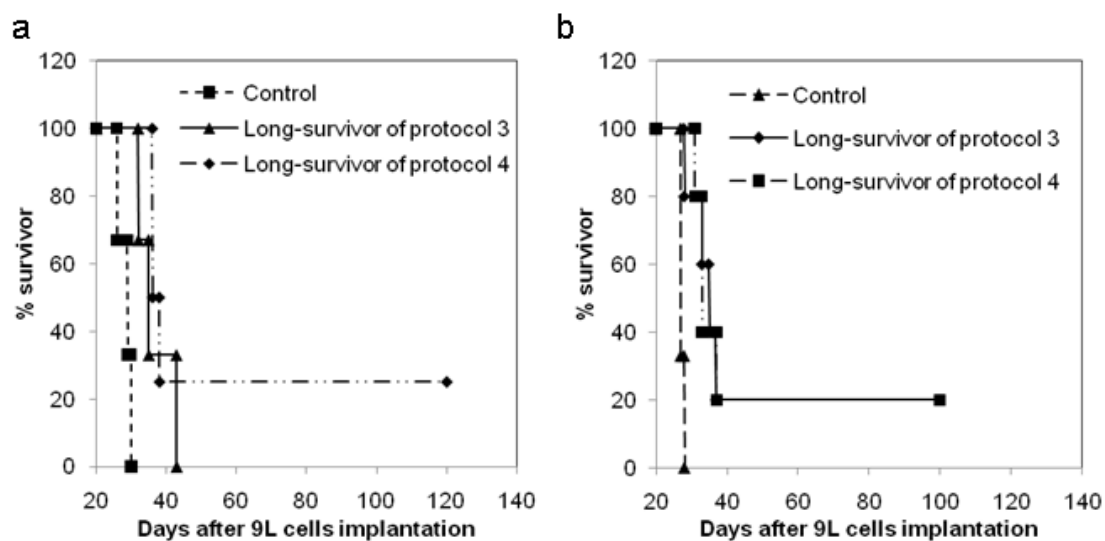
Figure 5:

Figure 5: Rechallenge in long-term survivors obtained from the nanovectorized internal radiation studies

a: Kaplan-Meier survival curves of re-challenged long-term survivors from the D6/D12 fractionated internal radiation study. **b**: Kaplan-Meier survival curves of re-challenged long-term survivors from the D12/D18 fractionated internal radiation study
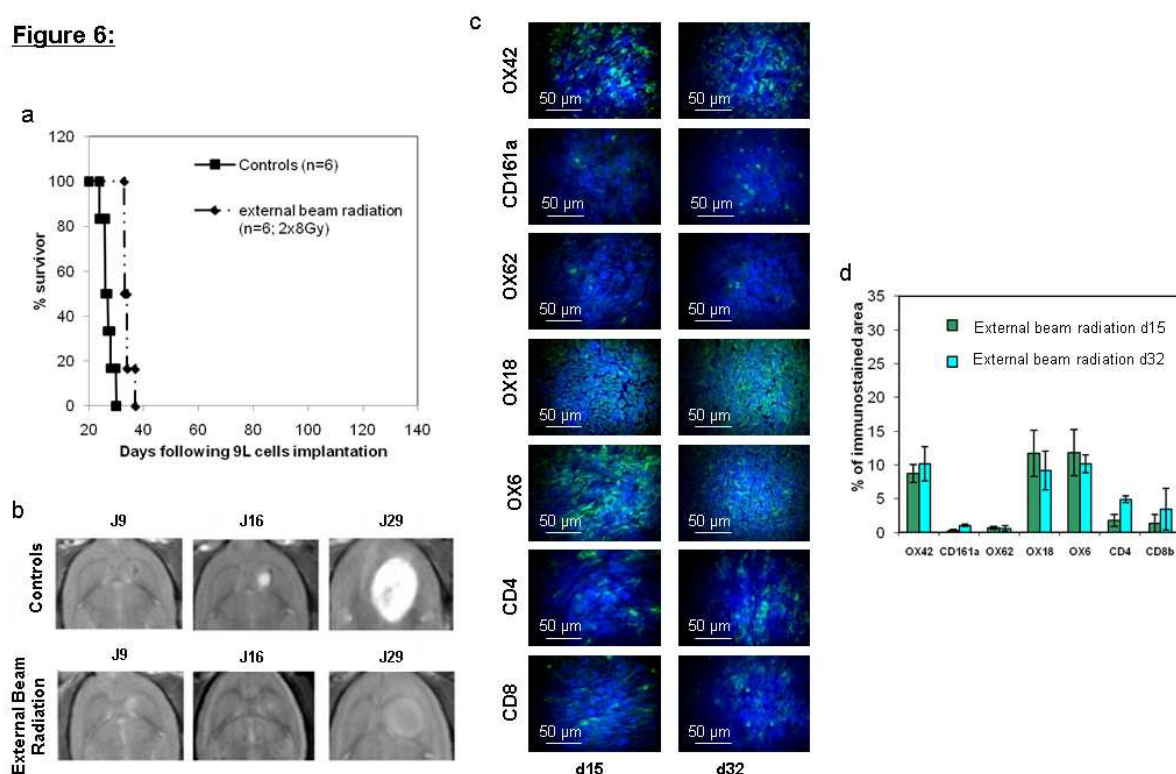
Figure 6: Efficacy of fractionated external beam radiation at D6 and D12 following tumor implantation and its immune system effects.

a: Kaplan-Meier survival curves of rats treated at D6 and D12with 2 x 8 Gy (n=6) and control animals (n=6). **b**: T2-weighted images of control and treated rats of the D6/external beam radiation study. **c**: Immunohistochemistry staining of macrophage cells (OX42), natural killer cells (OX61), major histocompatibility (class I - OX18; class II – OX6), dendritic cells (CD161a), and T lymphocytes cells (CD4 and CD8) of the D6/D12 external beam radiation study. **d**: Semi-quantitative results of immunohistochemistry. Results are expressed as % of immunostaining area after their determination with MetaMorph software.